The Intermediate Chain of Cytoplasmic Dynein Is Partially Disordered and Gains Structure upon Binding to Light-Chain LC8†

Afua Nyarko,‡,§ Michael Hare,‡ Thomas S. Hays,|| and Elisar Barbar*,‡

Department of Biochemistry and Biophysics, Oregon State University, Corvallis, Oregon 97331, Department of Chemistry and Biochemistry, Ohio University, Athens, Ohio 45701, and Department of Genetics, Cell Biology, and Development, University of Minnesota, Minneapolis, Minnesota 55455

Received July 20, 2004; Revised Manuscript Received September 10, 2004

ABSTRACT: The N-terminal domain of dynein intermediate chain, IC^{1-289}, is highly disordered, but upon binding to dynein light-chain LC8, it undergoes a significant conformational change to a more ordered structure. Using circular dichroism and fluorescence spectroscopy, we demonstrate that the change in conformation is due to an increase in the helical structure and to enhanced compactness in the environment of tryptophan 161. An increase in helical structure and compactness is also observed with trimethylamine-*N*-oxide (TMAO), a naturally occurring osmolyte used here as a probe to identify regions with a propensity for induced folding. Global protection of IC^{1-289} from protease digestion upon LC8 binding was localized to a segment that includes residues downstream of the LC8-binding site. Several smaller constructs of IC^{1-289} containing the LC8-binding site and one of the predicted helix or coiled-coil segments were made. IC^{1-143} shows no increase in helical structure upon binding, while $IC^{114-260}$ shows an increase in helical structure similar to what is observed with IC^{1-289}. Binding of $IC^{114-260}$ to LC8 was monitored by fluorescence and native gel electrophoresis and shows saturation of binding, a stoichiometry of 1:1, and moderate binding affinity. The induced folding of IC^{1-289} upon LC8 binding suggests that LC8 could act through the intermediate chain to facilitate dynein assembly or regulate cargo-binding interactions.

Cytoplasmic dynein is a 1.2-MDa minus-end-directed microtubule-associated motor protein complex that functions in a number of processes including organization and maintenance of the Golgi apparatus, nuclear migration, formation of the mitotic spindle, and the positioning and transport of organelles such as endosomes and lysosomes (*1*−*3*). The dynein complex is comprised of two 530-kDa heavy chains, two 74-kDa intermediate chains, two to four 50−60-kDa light intermediate chains and several 10−20-kDa light chains (*4*). The heavy chains are made up of globular domains responsible for ATPase and motor activities and slender stems that connect the motor domain to the rest of the complex and cargo through direct interaction with the intermediate chains. The 74-kDa intermediate chain (IC74)[1] and two light chains (LC8 and Tctex-1) form a tight subcomplex that remains associated in high salt concentrations (*5*−*7*).

The LC8 light chain is highly conserved with a greater than 90% amino acid identity between human, *Drosophila melanogaster*, and *Caenorhabditis elegans* light-chain subunits. The LC8 light chain is present in both axonemal and cytoplasmic isoforms of dynein and is also a subunit that interacts with several unrelated proteins including neuronal nitric oxide synthase, myosin V, the proapoptic factor Bim, and transcriptional factors Swallow and TRPS1 (*8*−*12*). The essential role of LC8 has been established by molecular genetics studies in several organisms (*13*, *14*) including *Drosophila*, where null mutations are lethal (*15*).

The intermediate chain IC74 is a key component of the cytoplasmic dynein complex. Molecular genetic analysis in *Drosophila* shows that mutations in the Dic gene result in larval lethality indicating that the intermediate chain also serves an essential function (*16*). In addition to acting as a scaffold for assembly of dynein subunits by associating directly with the heavy- and light-chain subunits, IC74 associates with several diverse proteins presumed to be cellular cargo. Examples include herpes simplex virus UL34 protein (*17*), PLAC-24 (*18*), the ClC-2 chloride channel (*19*), and β-catenin (*20*). IC74 interacts with the $p150^{Glued}$ subunit of dynactin, another multisubunit protein required for full cytoplasmic dynein activity (*21*, *22*). Dynactin is thought to mediate many dynein-related activities including its processivity along microtubules (*23*) and interactions with mitotic kinetochores (*24*, *25*) and organelles (*26*).

Sequence analyses and deletion mutations have identified two structurally and functionally independent domains of IC74, an N-terminal domain predicted to be primarily

† This work was supported by NSF CAREER Grant MCB-0417181 and NIH GM60969 to E.B. and NIH GM44757 to T.S.H.

* To whom correspondence should be addressed: Department of Biochemistry and Biophysics, Oregon State University, Corvallis, OR 97331. Telephone: 541-737-4143. Fax: 541-737-0481. E-mail: barbare@science.oregonstate.edu.

‡ Oregon State University.

§ Ohio University.

|| University of Minnesota.

[1] Abbreviations: LC8, 10-kDa dynein light chain; Tctex-1, 12.5-kDa dynein light chain; IC74, 74-kDa dynein intermediate chain; IC^{1-289}, IC^{1-143}, IC^{30-143}, and $IC^{114-260}$, constructs of *Drosophila* IC74 protein that include amino acids 1−289, 1−143, 30−143, and 114−260, respectively; GST, glutathione-*S*-transferase; ESI−MS, electrospray ionization mass spectrometry; CD, circular dichroism; TMAO, trimethylamine-*N*-oxide; TFE, 2,2,2-trifluoroethanol.

10.1021/bi048451+ CCC: $27.50
Published on Web 11/13/2004

unfolded (*27*) and a C-terminal domain composed of several WD40 repeats predicted to fold into a toroidal bladed β propeller (*28*). The N-terminal domain binds cargo, dynactin, and the light chains (*17*, *27*, *29*), while the C-terminal domain binds the heavy chain (*30*). A BLAST analysis of the two domains across species shows that the C-terminal domain is highly conserved with 66% sequence identity between *Drosophila* and human, while the N-terminal domain is less-conserved, with 25% sequence identity.

We have initiated studies into the interactions between the light chains LC8 and Tctex-1 and the intermediate chain IC74 in *Drosophila*. The N-terminal domain of IC74, IC^{1-289}, contains the binding site to both light chains (*27*, *31*, *32*). Using limited proteolysis followed by mass spectrometry, we localized the binding of the light chains to a short segment corresponding to residues 99−147 on the N-terminal domain (*27*). We further showed that IC^{1-289}, consistent with the prediction, is elongated and noncompact with limited secondary and tertiary structure near physiological conditions, but upon binding LC8 and, to a smaller extent, Tctex-1, IC^{1-289} becomes significantly more ordered. This increase in ordered structure is supported by an increase in global protection from proteolytic digestion and a change in the far-UV circular dichroism (CD) signal.

The view that a unique preformed three-dimensional structure is necessary for protein function has recently begun to change. Many proteins display functions requiring intrinsic disorder of the free protein (*33*). The importance of disorder has been established in the assembly of large complexes such as tobacco mosaic virus and flagellin (*34*). In the self-assembly of tobacco mosaic virus (*35*), the coat protein monomers have disordered loops located in the inner core of the virus. These highly flexible loops increase the entropic activation energy of binding and inhibit misassembly. On binding to RNA, these loops gain structure, resulting in the formation of a nucleating aggregate. In bacterial flagellum, the N- and C-terminal residues of flagellin are disordered in the monomeric form but undergo a large conformational change upon polymerization because of an increase in the α-helical content (*36*). Similarly, we suggest in this work that the proper assembly of the dynein complex requires both the flexibility and adaptability inherent in free disordered IC^{1-289} and a productive encounter with LC8. We use smaller constructs of IC^{1-289} to identify the segments that gain structure upon LC8 binding and show that the induced structural change is due to an increase in the helical structure in residues distant from the LC8-binding site. We further characterize the specificity and stoichiometry of the LC8−IC interactions and the induced compactness that accompanies these interactions.

EXPERIMENTAL PROCEDURES

Overexpression and Purification of LC8 and IC74 Constructs. The cDNA (accession number AF263371) encoding the full-length *Drosophila* cytoplasmic dynein intermediate chain was used as the template in PCR reactions to generate several constructs: IC^{1-289}, IC^{1-143}, IC^{30-143}, and $IC^{114-260}$ with either *Bam*H1−*Hin*dIII or *Bam*H1−*Sal*1 restriction sites. The PCR products were subcloned into pET 15d expression vectors with a polyhistidine tag (Novagen) and transformed into BL21 (DE3) bacterial expression cell lines (Invitrogen).

Protein expression and purification for IC^{1-289} followed protocols described elsewhere (*27*). For expression of IC^{1-143}, IC^{30-143}, and $IC^{114-260}$, a 5 mL overnight culture of the recombinant BL21 (DE3) grown at 37 °C was used to inoculate a 1 L of LB medium containing 100 μg/mL ampicillin, and growth continued until $OD_{600} = 0.6$. Protein expression was induced by isopropyl-β-D-thiogalactosidase (IPTG) at a final concentration of 0.4 mM, and growth continued at 27 °C for 5 h. Cells were harvested and lysed by sonication. The cell debris was removed by centrifugation at 18 000 rpm in a Beckman JA21 rotor for 30 min. The soluble polyhistidine-tagged proteins were purified on a Ni-NTA-affinity column (Qiagen). Protein purity was confirmed on a 15% SDS−PAGE, and the molecular mass of each protein was determined by mass spectrometry. LC8 and glutathione-*S*-transferase (GST)-fused LC8 for GST pull-down assays were prepared following methods described earlier (*37*).

Site-Directed Mutagenesis. Site-directed mutagenesis of the single tryptophan (TGG) at position 54 of LC8 to phenylalanine (TTC) was done following the GeneEditor *in vitro* protocol (Promega) and using the mutagenesis oligonucleotide 5′-pTAC AAT CCC ACA T**TC** CAT TGC ATT GTC GGT C-3′. The mutant DNA was verified by sequencing before transformation into BL21 (DE3) cell lines for protein expression.

Protein Concentrations. Protein concentrations were determined from absorbance at either 280 or 500 nm. For absorbance at 280 nm, the Beer−Lambert relationship was used with molar extinction coefficients (IC^{1-289}, 22 900; $IC^{114-260}$, 14 650; LC8, 13 370; and W54F LC8, 7680 M^{-1} cm^{-1}) obtained from ProtParam (http://us.expasy.org/tools). For absorbance at 500 nm, the method of Lowry et al. (*38*) as modified by Peterson (*39*) was used with bovine serum albumin as the standard. With the exception of IC^{1-143}, which has a low molar extinction coefficient (2560 M^{-1} cm^{-1}), all of the proteins gave similar concentration values with both methods.

Limited Proteolysis, In-Gel Digestion, and Mass Spectrometry. Limited proteolysis of the intermediate chain constructs, LC8, and the IC−LC8 complex were performed at 4 °C with proteinase K (Novagen) as described previously (*27*, *37*). The protected fragments were excised from the SDS−PAGE gel and transferred to 1.5 mL tubes prewashed with 0.1% trifluoroacetic acid (TFA) in 60% acetonitrile. A blank section of the gel was used as a control. Cut gels were washed successively with 50% acetonitrile in 50 mM NH_4HCO_3 and 50% acetonitrile in 10 mM NH_4HCO_3. Tryptic digestion was performed on the gel pieces in 10 mM NH_4HCO_3 at pH 8 at 37 °C for 24 h. The resulting tryptic peptides were extracted with 0.1% TFA in 60% acetonitrile and lyophilized.

Mass spectrometric data were acquired using a Bruker Esquire electrospray ionization system. Samples were prepared for analysis by redissolving lyophilized peptides in 5% acetonitrile/0.05% TFA. Peptides were identified by comparing the mass of the fragments (±1 amu) with the masses of all possible tryptic digest sequences within IC^{1-289}.

CD Spectropolarimetry. CD experiments were recorded on a JASCO 715 spectropolarimeter, equipped with a Peltier type cell holder for temperature regulation. All of the reactions were done at 25 °C with protein concentrations of

5−8 μM in 10 mM sodium phosphate/10 mM NaCl at pH 7.8. CD spectra were recorded in a 1 mm cell using 0.5 nm step resolution and 1.0 nm bandwidth, and three scans were averaged for each run.

Data for TMAO or trifluoroethanol (TFE) (Sigma) experiments were acquired after incubating the proteins for 5 min in 10 mM sodium phosphate buffer containing different concentrations of either TMAO or TFE. The difference spectra representing the bound IC constructs were obtained by subtracting a spectrum of equimolar concentration of LC8 from the spectrum of the mixture. The percent helicity values were determined using K2D neural network analysis, which shows good performance in the 200−240 nm wavelength range (*40*).

Fluorescence Spectroscopy. The intrinsic fluorescence emission spectra of $IC^{114-260}$ free or bound to W54F LC8 were acquired on a Jobin Yvon/Spex spectrofluorometer using a 0.5 cm quartz cuvette. Samples were prepared by treating 8 μM $IC^{114-260}$ in 50 mM sodium phosphate buffer at pH 7.8, with increasing concentrations of W54F LC8 and incubating the mixture for 1 h at 25 °C. The excitation wavelength was set to 295 nm to selectively excite tryptophan residues, and emission was recorded between 310 and 380 nm using a scan speed of 1 nm/s and excitation and emission slit widths of 5 and 6 nm, respectively, at 25 °C. Fluorescence contributions of the buffer and the W54F LC8 were recorded and subtracted for each data point. Experiments in TMAO were recorded after incubating IC^{1-289} or $IC^{114-260}$ in 0.32−2.4 M TMAO prepared in 50 mM sodium phosphate buffer at pH 7.8. Corrections for contributions of the buffer and TMAO were made as before.

Native Gel Shift Assay. To determine binding stoichiometry, a constant concentration of 10 μM of $IC^{114-260}$ in 50 mM sodium phosphate at pH 7.8 was titrated with increasing concentrations of LC8 ranging from 0.17 to 30 μM. The proteins were separated on a 15% acrylamide (29:1) gel, prepared according to the method of Laemmli (*41*) without SDS, using a constant current of 6 mA and a 25 mM Tris/19.5 mM glycine buffer. Bands were visualized with Coomassie Blue stain, and their intensities were estimated with Quantity-one quantitation software (Bio-Rad Laboratories).

Analytical Ultracentrifugation. Sedimentation velocity and equilibrium data were collected using a Beckman Optima XL-A analytical ultracentrifuge. For sedimentation velocity, a rotor speed of 40 000 rpm was used for two protein concentrations. For equilibrium experiments, three loading concentrations were equilibrated at two speeds (28 000 and 40 000) and scanned at 230 nm using a cell path length of 3 mm. All experiments were done at 4 °C.

Structure Prediction. Coil (*42*) was used to predict residues in the coiled-coil conformation and Multicoil (*43*) to determine the probability of the coiled-coil to be di- or trimeric. The secondary structure was predicted with PSIPRED (*44*).

RESULTS

Increase in Secondary Structure of IC^{1-289} upon LC8 Binding. A comparison of the far-UV CD spectra of free IC^{1-289} with the spectrum of LC8-bound IC^{1-289} (obtained by subtracting the signal of free LC8 from the spectrum of the LC8−IC^{1-289} complex) indicates a significant structural change upon binding (Figure 1). Free IC^{1-289} (□) has a weak signal at 222 nm and a stronger signal at 204 nm, indicative of a primarily unfolded protein, while the LC8-bound IC^{1-289} shows a shift of the CD signal at 204 nm toward 208 nm and a considerable increase in the negative ellipticity at 220 nm (■). The value of $[\Theta_{222}]/[\Theta_{208}]$ increases from 0.66 for the free to 0.96 for the bound protein. A typical $[\Theta_{222}]/[\Theta_{208}]$ value for noncoiled-coil α helices is 0.83, while values close to 1 are observed for coiled-coil helices (*45*). There is a 2-fold increase in percent helicity, from 9% in the unbound protein to 17% in the bound, as calculated by K2D (*40*). These observations suggest that upon binding to LC8, a segment of IC^{1-289} assumes a helical conformation with possible supercoiling. When the difference spectra are analyzed, the assumption is made that the change in average CD structure is primarily due to a conformational change in IC^{1-289} and not in LC8. This is a plausible assumption because LC8 is a stable folded protein (*46*) and therefore not likely to undergo significant secondary structural changes upon binding. These data are similar to our earlier report (*27*), but here, the experiment is designed to facilitate the computation of difference spectra for direct comparison of IC^{1-289} in the free and bound states (see the Experimental Procedures).

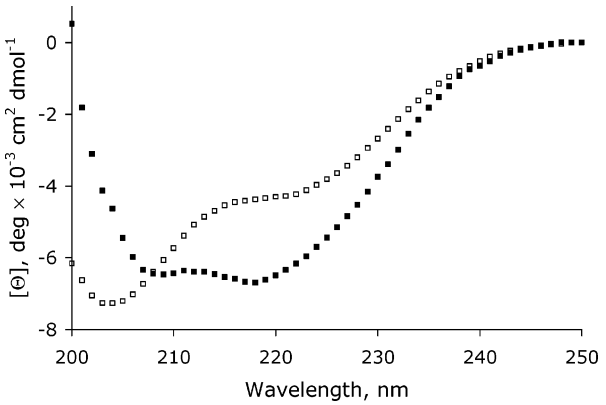

FIGURE 1: Increase in the secondary structure of IC^{1-289} upon LC8 binding monitored by CD spectroscopy. Far-UV CD spectra were collected at 25 °C for free IC^{1-289} (□) and IC bound to LC8 (■) in 10 mM sodium phosphate and 10 mM NaCl at pH 7.8. The spectrum of bound IC^{1-289} was generated by subtracting the spectrum of LC8 from the spectrum of the complex of IC^{1-289} and LC8. Protein concentrations were 6 μM for both IC^{1-289} and LC8.

Increase in Ordered Structure of IC^{1-289} by an Osmolyte. CD spectra of IC^{1-289} recorded in the absence (□) and in 2.4 M (■) TMAO (Figure 2A) show an increase in negative ellipticity at 222 nm, a wavelength shift from 204 to 208 nm, and an increase in the value of $[\Theta_{222}]/[\Theta_{208}]$ from 0.66 for the protein without osmolyte to 0.90 in 2.4 M TMAO. These observations indicate an increase in the secondary structure in the presence of TMAO. The inset in Figure 2A shows a plot of the relative increase in negative ellipticity at 222 nm as a function of the TMAO concentration. The data were normalized such that the negative ellipticity for the protein in 0 M TMAO is given a value of 0 and the negative ellipticity in 2.4 M TMAO is given a value of 1. The increase in ellipticity reaches saturation at a TMAO concentration somewhat over 1.5 M. A similar increase in the helical structure is observed with TFE (data not shown).

Fluorescence emission spectra of constant concentration of IC^{1-289} collected at increasing concentrations of TMAO show a blue shift in the emission maximum from 350 nm in

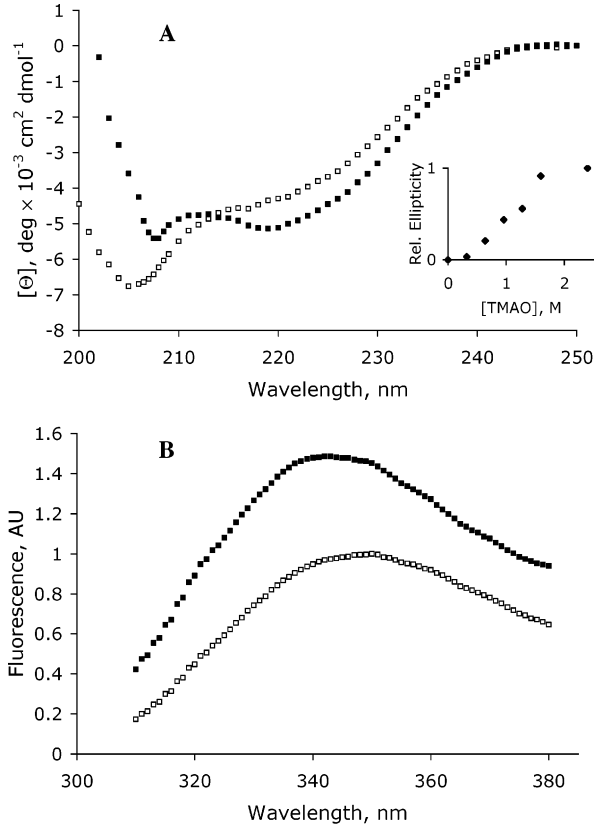

FIGURE 2: Increase in the structure of IC^{1-289} in TMAO. (A) Far-UV CD spectra of 6 μM IC^{1-289} in 0 M (□) and 2.4 M (■) TMAO. The inset shows a relative CD signal at 222 nm of IC^{1-289} as a function of the TMAO concentration, where the signal in 0 M TMAO is given a value of zero. TMAO concentrations were 0, 0.32, 0.64, 0.96, 1.28, 1.60, and 2.40 M. All of the CD experiments were recorded at 25 °C in 10 mM sodium phosphate and 10 mM NaCl buffer at pH 7.8. (B) Fluorescence emission spectra of 6 μM IC^{1-289} in 0 M (□) and 2.4 M (■) of TMAO. There is a blue wavelength shift of the maximum intensity from 350 nm as the concentration of TMAO increases and reaches saturation at 342 nm.

the absence of TMAO to 342 nm in 2.4 M TMAO and a substantial enhancement in intrinsic fluorescence indicating that TMAO induces some condensed structure in IC^{1-289} (Figure 2B). The saturation observed above 1.5 M TMAO suggests that the increase in the CD-detected structure and compactness occurs only in a small segment of IC^{1-289}, while the majority of the protein remains disordered.

Identification of Fragments of IC^{1-289} that Are Globally Protected upon LC8 Binding. Three distinct bands migrating at approximately 20, 26, and 30 kDa are less susceptible to digestion by proteinase K in the presence of LC8 than when LC8 is absent (see Figure 1 in ref 37). Here, we have extracted these bands by in-gel trypsin digestion and identified their component peptides by electrospray mass spectrometry (Table 1). The fragment migrating at 30 kDa includes peptides that span the sequence 105−288 (lines 1−6 of Table 1). The calculated molecular mass for residues 105−288 is 20.7 kDa. The difference between the calculated and estimated mass from SDS−PAGE is observed in all of our experiments with IC74 fragments. For example, IC^{1-289} has a calculated mass of 33 kDa but migrates at 43 kDa, and similarly, a fragment with a mass of 13 kDa migrates at 20 kDa (*27*). This slow migration rate has been observed in other

Table 1: ESI−MS Identification of Peptides from In-Gel Tryptic Digestion of Protected Fragments of IC1-289 in the Presence of LC8

apparent masses on gel	observed mass[a] (Da)	theoretical mass[b] (Da)	residues[c]
30 kDa	987.5 (2960.5)	2960.4	105−130
	747.6 (1494.2)	1493.8	184−197
	957.6 (2870.8)	2870.4	184−210
	1094.2 (3280.6)	3280.7	211−239
	602.6	602.7	278−282
	828.8	828.9	283−288
26 kDa	733.6	733.4	210−215
	667 (1333.6)	1333.4	216−226
	690.3 (1379.6)	1378.6	227−237
	602.6	602.3	278−282
20 kDa	747.7 (1494.6)	1493.8	184−197
	698.5 (1396.0)	1395.7	198−210

[a] The number in parentheses is the observed mass after correction for multiple charge states. [b] Theoretical mass is based on the composition of the peptide. [c] Residues were identified by the match of masses of possible tryptic fragments with the observed mass.

intrinsically disordered proteins and attributed to the high proportion of negatively charged residues, which can restrict the binding of SDS and result in an apparent molecular weight 1.2−1.8 times higher than the real one calculated from the sequence (*47*, *48*). Therefore, the fragment that migrates as 30 kDa according to a PAGE standard obtained with known proteins is actually closer to 20 kDa than to 30 kDa and may include a few residues N terminal to 105. The few peptides identified for fragments migrating at 26 kDa (lines 7−10 of Table 1) and 20 kDa (lines 11−12 of Table 1) appear to correspond to secondary digests of the 30-kDa fragment. From these results, we conclude that there is no evidence of protection for the first 80−100 residues of IC74 in the presence of LC8.

Design and Characterization of Smaller Constructs of IC^{1-289}. IC^{1-289} is significantly depleted in most "order-promoting" residues (Trp, Cys, Phe, and Ile) and enriched in some "disorder-promoting" residues (Glu and Lys) compared with the average values in the Swiss Protein database (Figure 3A), consistent with a disordered protein. Sequence analysis using MultiCoil (*43*) predicts that residues 1−30 form a dimeric coiled coil, while residues 209−237 show a small tendency to form a trimeric coiled coil. PSIPRED (*44*) predicts two short helices spanning residues 2−37 and 223−250, while the rest of the protein is random (Figure 3B). On the basis of these predictions, we prepared two constructs IC^{1-143} and $IC^{114-260}$, each containing the LC8-binding site (residues 114−143) and one of the regions predicted to contain a coiled coil or helix. IC^{30-143}, which contains the LC8-binding site but lacks a predicted coiled-coil or helix sequence, was also prepared for comparison. The molecular masses of the purified proteins determined from mass spectrometry are in agreement with their calculated masses: IC^{1-143}, 17 139.9 amu (17 138.8 calculated); $IC^{114-260}$, 18 114 amu (18 115.8 calculated).

Binding of each construct to LC8 was confirmed by a GST pull-down binding assay, using LC8 fused to GST (lanes 4 and 5 of Figure 4). Far-UV CD spectra of various IC constructs are shown in Figure 5. All constructs are primarily unfolded with a varying percentage of helical conformation present. IC^{1-143} (△) has the highest helical content of 23%, consistent with 20% of the coiled-coil (residues 2−30) and

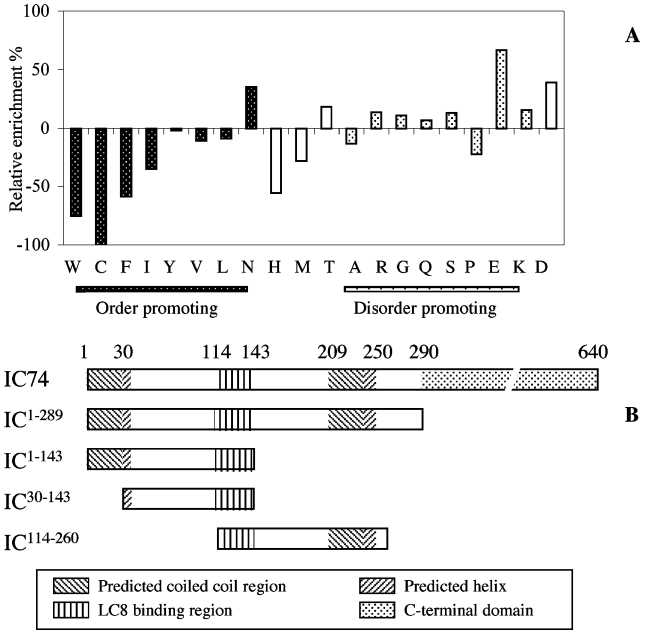

FIGURE 3: (A) Deviation in amino acid composition from the average values in the Swiss-Prot database of residues 1−288. The relative enrichments of order promoting (dark bars), disorder promoting (dotted bars), and neutral (white bars) are shown. (B) Schematic representations of constructs of IC74 used in this work. IC74 is comprised of two structurally and functionally independent domains (1−289 and 290−640). The N-terminal domain contains two predicted coiled-coil regions (1−30 and 209−239), two predicted helices (2−37 and 223−250), and a binding region for LC8 (114−143). Constructs were designed to include the LC8-binding region and either the first coiled-coil segment, IC^{1-143}, or the second coiled-coil and helical segment, $IC^{114-260}$.

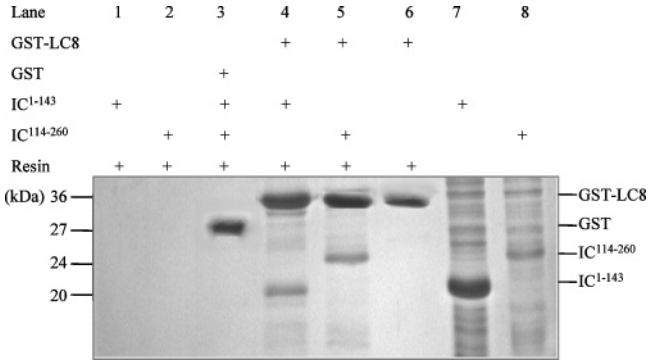

FIGURE 4: GST pull-down assays showing the interaction of GST fused to LC8 with IC^{1-143} and $IC^{114-260}$ from crude lysate extracts. Lanes 4 and 5 correspond to lysates of IC^{1-143} and $IC^{114-260}$ mixed with glutathione sepharose 4B resins and GST−LC8. The presence of IC^{1-143} and $IC^{114-260}$ bands indicate binding. For negative controls, lysates of IC^{1-143} and $IC^{114-260}$ were incubated with GST-conjugated resins (lane 3) and with only the resins (lanes 1 and 2) to rule out nonspecific binding to GST or the resin. A band for the constructs only appears with GST−LC8 indicating specific binding (lanes 4 and 5). Lanes 7 and 8 show crude cell lysates of His-tagged IC^{1-143} and $IC^{114-260}$.

helix (residues 3−37) predictions. A comparison of IC^{1-143} (△) to IC^{30-143} (×, helical content 4%) verifies that most of the helical structure observed in IC^{1-143} is indeed contributed from the first 30 residues. The shape of IC^{1-289} spectrum (●) is similar to that of IC^{1-143}, indicating that most of the structure in IC^{1-289} is also contributed from the first 30 residues. The spectrum of $IC^{114-260}$ (○), with a minimum at 202 nm, indicates that this construct is completely disordered

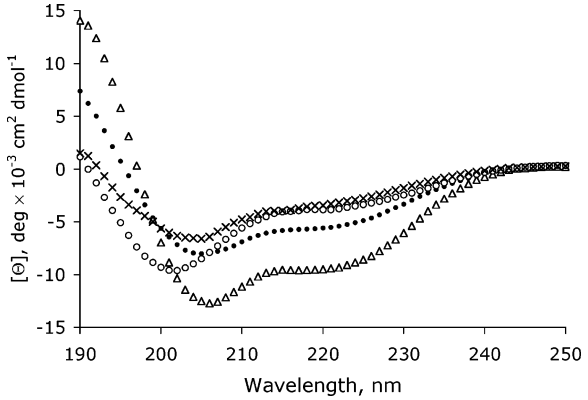

FIGURE 5: Far-UV CD spectra of IC^{1-289} (●), IC^{1-143} (△), IC^{30-143} (×), and $IC^{114-260}$ (○) shown in molar ellipticity. Spectra were acquired at 25 °C using protein concentrations of 8 μM in 10 mM sodium phosphate buffer and 10 mM NaCl at pH 7.8.

with no detectable helical content. About 18% of the protein sequence is predicted to fold as coiled-coil (residues 209−237) or helix (residues 223−250).

Hydrodynamic analysis using sedimentation ultracentrifugation and size-exclusion chromatography show that $IC^{114-260}$ is an elongated nonglobular monomeric protein. Sedimentation velocity measurements performed at 4 °C at 40 000 rpm showed that $IC^{114-260}$ is a single component with an s (20,w) of approximately 1.5 s. Sedimentation equilibrium performed at 40 000 and 28 000 rpm and three protein concentrations gave an apparent molecular mass of 18 140 Da in close agreement with the calculated molecular weight of 18 115 Da. A single peak was also observed by size-exclusion chromatography but with a larger Stoke's radius than expected for globular proteins of similar mass, consistent with an elongated nonglobular monomer (data not shown).

Binding of Small IC Constructs to LC8. Far-UV CD spectra were obtained for IC^{1-143} (Figure 6A) and $IC^{114-260}$ (Figure 6B) in the presence (■) and absence (□) of LC8. Upon LC8 binding, a significant change in the spectrum consistent with an increase in the helical structure is observed with $IC^{114-260}$ but not with IC^{1-143}. An increase in the negative molar ellipticity at 222 nm, a shift from 203 to 207 nm, and an increase in the value of $[\Theta_{222}]/[\Theta_{208}]$ from 0.45 to 1 are observed in bound $IC^{114-260}$ (Figure 6B). These changes are similar to those observed in bound IC^{1-289} (Figure 1). The increase in secondary structure (percentage helix of 13% in the bound) observed only in $IC^{114-260}$ strongly suggests that the residues C terminal to the LC8-binding site that are predicted to be helical or coiled-coil are necessary and perhaps sufficient for the observed change in conformation in IC^{1-289} upon LC8 binding.

To determine the stoichiometry of binding, a constant concentration of $IC^{114-260}$ was incubated with increasing concentrations of LC8 and the formation of the complex was visualized using native gel electrophoresis. Figure 7 shows migration of $IC^{114-260}$ (lane1), LC8 (lane 2), and a mixture of the two proteins in IC/LC8 molar ratios increasing from 1:0.125 to 1:4 (lanes 3−10). Before complex formation, both proteins migrate at similar rates on the gel. While $IC^{114-260}$ is considerably more expanded than the LC8 dimer, its low calculated pI of 4.9 relative to 7.0 for LC8 contributes to their similar migration rate. Lanes 3−6 show a higher molecular weight band representing the complex of $IC^{114-260}$

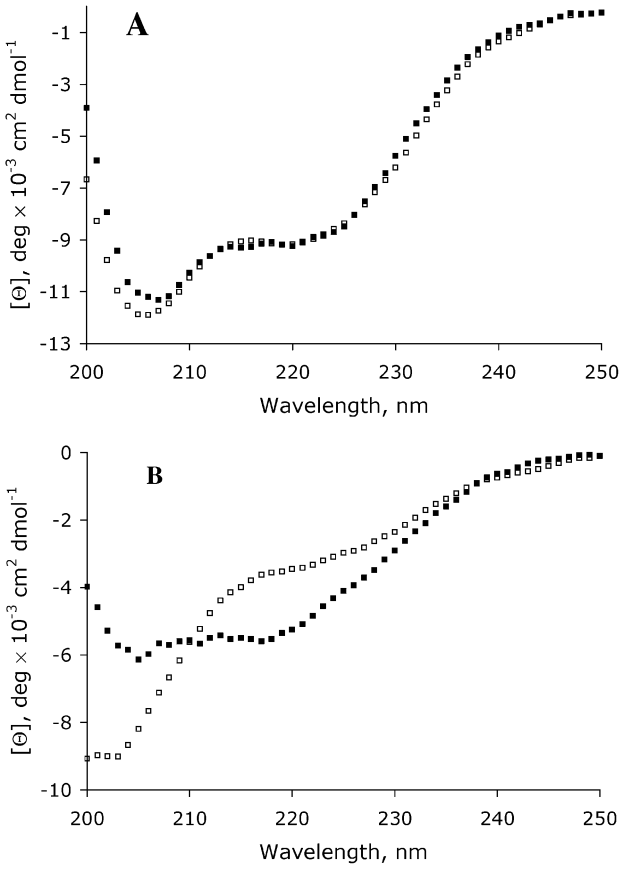

FIGURE 6: Far-UV CD spectra of (A) IC^{1-143} and (B) $IC^{114-260}$ free and bound to LC8. Spectra of free IC^{1-143} and $IC^{114-260}$ are shown in □, while LC8-bound are shown in ■. There is no significant difference between free and bound (A) IC^{1-143}, while there is considerable difference between free and bound (B) $IC^{114-260}$. Protein concentrations were 6 μM for IC^{1-143} and 8 μM for $IC^{114-260}$ and LC8, in 10 mM sodium phosphate and 10 mM NaCl buffer at pH 7.8. Spectra for the bound proteins were generated as explained in the Experimental Procedures.

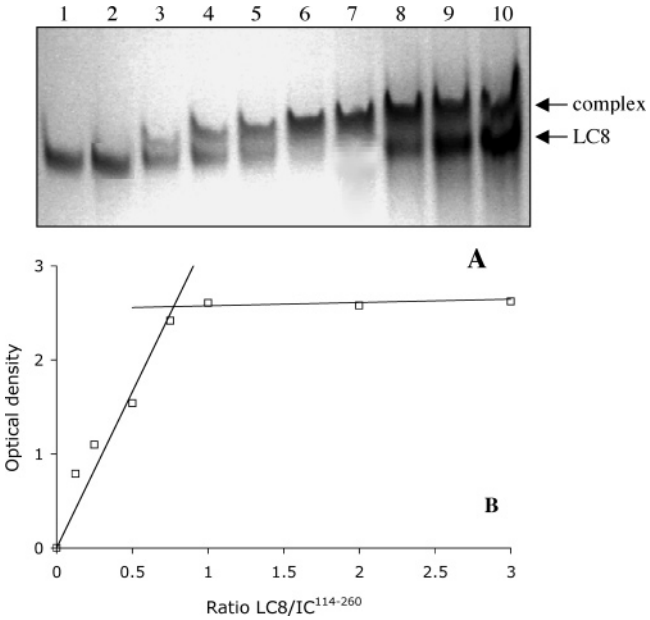

FIGURE 7: (A) Titration of a constant concentration of 10 μM $IC^{114-260}$ with an increasing concentration of LC8 monitored by native PAGE. Lanes 1 and 2 represent 10 μM of $IC^{114-260}$ and LC8, respectively, and lanes 3−10 represent mixtures of $IC^{114-260}$ and LC8 in the ratios of 1:0.125, 1:0.25, 1:0.5, 1:0.75, 1:1, 1:2, 1:3, and 1:4. (B) Plot of the intensities of the bands corresponding to the complex as a function of the molar ratios of $IC^{114-260}$ and LC8. Extrapolation of the intersection of the two slopes to the abscissa yields the moles of LC8 bound per mole of $IC^{114-260}$ (close to 1). The bands of the complex were analyzed with the Quantity-one quantitation software (Bio-Rad).

and LC8 and a lower molecular weight band representing $IC^{114-260}$. A band for free LC8 is not observed because $IC^{114-260}$ is in molar excess. Lane 7, which corresponds to an equimolar concentration of the two proteins, shows a single band for the complex. Lanes 8−10 with LC8 in molar excess show bands corresponding to the complex and free LC8.

A representative plot of the three native gels analyzed shows the quantified intensities of the complex as a function of the LC8/$IC^{114-260}$ molar ratio (Figure 7B). The maximum complex formation is attained at a molar ratio close to 1, indicating saturation of binding and a binding stoichiometry of 1:1. The molar ratios of the proteins were calculated based on their monomeric concentrations. At higher concentrations, LC8 is a dimer with a K_d of 11 μM (*46*) and hence binds two units of monomeric $IC^{114-260}$. The decrease in the migration rate of the complex at a higher concentration of LC8 (lane 7 relative to lane 3) may be explained by an increase in the population of dimeric LC8, resulting in a complex of two units of LC8 and two units of $IC^{114-260}$.

To facilitate fluorescence studies of LC8−$IC^{114-260}$ interactions, the single tryptophan in LC8, Trp54, was replaced by phenylalanine. This mutation did not perturb its binding to $IC^{114-260}$ as verified by a GST pull-down assay (data not shown). The single tryptophan in $IC^{114-260}$, Trp161, is considerably exposed to the solvent as indicated by an emission maximum of 350 nm (Figure 8, inset, □). The emission intensity at 350 nm of 8 μM $IC^{114-260}$ is enhanced in the presence of increasing concentrations of LC8W54F and reaches saturation at about 8 μM, indicating that binding is specific with a stoichiometry of 1:1. The significant increase in fluorescence intensity is accompanied by a blue shift to 343 nm, suggesting that Trp161 becomes buried upon LC8 binding (Figure 8, inset, ■). Similar changes in fluorescence spectra are observed for IC^{1-289} upon LC8 binding (data not shown). The increase in compactness in $IC^{114-260}$ and IC^{1-289} indicates that the part of the protein that becomes more folded is within residues 114 and 260. At a lower concentration (4 μM), a similar increase in fluorescence intensity and 1:1 binding stoichiometry was also observed (data not shown). Global fitting of the data at both concentrations gave a dissociation constant in the submicromolar range, 90 ± 200 nM. The large uncertainty is due to the limited number of points that could be collected before saturation, because of the tight binding at the concentrations needed for this experiment.

DISCUSSION

CD, fluorescence, and sedimentation velocity demonstrate that IC^{1-289} is disordered at physiological temperature and pH, but upon addition of LC8, it gains CD-detected secondary structure and becomes more resistant to proteolysis (*27*, *37*). Our goal in this work is to characterize the conformational changes upon LC8 binding and identify the sequence on IC^{1-289} that is responsible for the change.

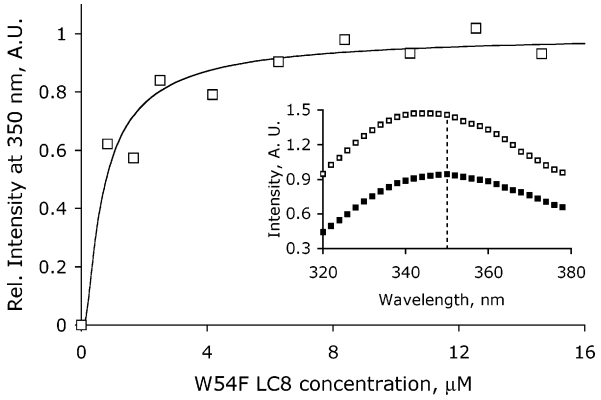

FIGURE 8: Titration of a constant concentration of 8 μM $IC^{114-260}$ with an increasing concentration of LC8W54F, monitored by relative fluorescence intensity at 350 nm. Fluorescence intensity was normalized to 0 in the absence of LC8 and 1 in the presence of a 3-fold excess. The curve is drawn to guide the eye and is not based on a binding model. The inset shows fluorescence emission spectra of free $IC^{114-260}$ (■) and a 2:1 mixture of LC8/$IC^{114-260}$ (□). The increase in intensity and a shift in λ_{max} from 350 to 343 nm indicate an increase in the compact structure of $IC^{114-260}$. Data were acquired on a Jobin Yvon/Spex spectrofluorometer using excitation and emission slit widths of 5 and 6 nm, respectively. All experiments were conducted at 25 °C in 50 mM sodium phosphate buffer at pH 7.8. Excitation was done at 295 nm to selectively excite the single tryptophan in $IC^{114-260}$. The spectrum of LC8W54F was subtracted from the spectrum of the mixture at every protein concentration to remove minor contributions from tyrosine and phenylalanine emission.

The increase in negative ellipticity of IC^{1-289} at 222 nm caused by binding to LC8, as well as the wavelength shift from 204 to 208 nm (Figure 1) indicate formation of an α helix. The possible presence of a coiled coil is reflected in the increase of $[\Theta_{222}]/[\Theta_{208}]$. The addition of the osmolyte TMAO causes changes in the spectra of IC^{1-289} similar to those obtained upon LC8 binding (Figure 2). This suggests that, while free IC^{1-289} is unfolded in its native state, it has a short segment with a propensity for helix formation, which is triggered with addition of either LC8 or TMAO. TMAO is a naturally occurring organic osmolyte that is found in water-stressed organisms, which at high or variable concentration, prevent proteins from unfolding, aggregating, and losing functional activity when exposed to environmental stresses such as extreme temperatures and high salt concentrations (*49*). It is commonly used as a reagent to induce folding of destabilized proteins *in vitro* and restore their biological activity to mimic their native conformation (*50*, *51*). Naturally occurring osmolytes such as TMAO do not change the rules for folding, they simply raise the free energy of the denatured state, thus making the folded state more favorable. Fluorescence studies with TMAO confirm a change in tertiary packing and an increase in compactness in the vicinity of Trp161. Therefore, because LC8 and TMAO induce similar structural changes, it is likely that the structure of IC^{1-289} when assembled in dynein reflects the structure stabilized by TMAO or LC8, which is somewhat condensed, with few short helices (17% of the structure) and long disordered segments.

Proteinase K, a nonspecific enzyme that cleaves exposed and flexible amide bonds, was used to identify the segment of IC^{1-289} that undergoes a global change in conformation in the presence of LC8 (*37*, *52*). The protected segment corresponds to residues 105−288, which include the LC8-binding site (114−143) and residues 209−250, which are predicted to fold into a weak trimeric coiled-coil followed by an α helix. All other smaller protected fragments include residues 209−250, while residues 1−30 that are predicted to fold into a dimeric coiled-coil or helix are not protected upon LC8 binding (Table 1).

To determine whether any of the predicted helix or coiled-coil segments contribute to the increase in ordered structure upon LC8 binding, constructs containing the LC8-binding site and one of the predicted helices or coiled-coils were prepared and their binding to LC8 was compared to that of IC^{1-289}. CD spectra of IC^{1-143} are consistent with residues 1−30 being helical, while CD spectra of $IC^{114-260}$ show no evidence of a folded structure (Figure 5), indicating that residues 209−250 are unable to form a helix or a coiled-coil on their own. Interestingly, upon addition of LC8, $IC^{114-260}$ gains a structure similar to the gain observed for IC^{1-289} (Figures 1 and 6), verifying that folding of a segment within residues 114−260 contributes to the increase in helical structure. A more compact structure is induced upon LC8 binding as monitored by an increase in fluorescence intensity and a blue shift in emission maximum wavelength (Figure 8). Fluorescence and native gel electrophoresis show that binding is specific, moderately tight, and with a stoichiometry of 1:1 (Figures 7 and 8).

The interesting conclusion from these studies is that the N-terminal domain of IC74 is disordered, but upon LC8 binding, it gains helical structure and becomes more condensed, specifically in a segment distant from the LC8-binding site. Residues 209−250 that are predicted to be coiled-coil and helix are in fact unfolded when free but become helical when LC8 binds IC ∼100 residues upstream, while the rest of the protein remains unfolded.

The combination of low overall hydrophobicity and large net charge in IC^{1-289} indicates little tendency for folding into a hydrophobic core. The folding process is then incomplete for free IC^{1-289} and proceeds further only by having the right partners with which to assemble. Because large complexes cannot be assembled from rigid components, the flexibility of the N-terminal domain of IC74 and its induced folding may be instrumental for regulating the assembly of the dynein complex. We speculate that LC8 binding may affect dynein heavy-chain function through direct binding and inducing folding of the intermediate chain. While the binding to the heavy chain is mapped to the C-terminal domain of IC74, residues 107−278 that contain the LC8-binding site and the sequence that changes conformation upon binding are also necessary for stable association with the heavy chain (*30*). Genetic experiments on filamentous fungi support a role for LC8 in mediating the function of the dynein heavy-chain (*53*), where a deletion mutation of the LC8 gene results in defects similar to the dynein heavy-chain null mutants. It will be interesting to test whether LC8 regulates binding of proteins that interact with IC74 at or close to the segment that changes conformation. Recent biochemical evidence has shown that the IC74 subunit binds directly to the two light chains of the kinesin I motor complex (*54*). Interestingly, the IC domain required for kinesin light-chain binding also includes residues 209−250 (*54*) that are responsible for the increase in structure upon LC8 binding. This region of the intermediate chain is also close to the binding site of the

roadblock dynein light-chain subunit, which includes residues 251−289 in *Drosophila* IC (*55*).

A role for LC8 as a molecular glue or stabilizer has been suggested by its presence in complexes unrelated to dynein (*4*). We have shown that binding of LC8 to the Swallow protein, a transcription factor presumed to be a dynein cargo, indeed promotes its assembly into a dimeric coiled-coil that is otherwise a partially folded monomer in the physiological temperature range (*56*). Our present analysis shows a similar increase in structure in IC74 upon LC8 binding. These studies taken together suggest that an increase in the ordered structure of protein substrates that bind LC8 may underlie the mechanism by which LC8 contributes to complex stabilization.

ACKNOWLEDGMENT

We acknowledge the support of the nucleic acid and protein core and the mass spectrometry facilities and services core in the Oregon State University Environmental Health Sciences Center (NIH/NIEHS 00210) and Dr. Lei Wang for performing the site-directed mutagenesis of LC8.

REFERENCES

1. Vaisberg, E. A., Koonce, M. P., and McIntosh, J. R. (1993) Cytoplasmic dynein plays a role in mammalian mitotic spindle formation, *J. Cell Biol. 123*, 849−858.
2. Harada, A., and Hirokawa, N. (1999) The role of cytoplasmic dynein in the ER to Golgi transport, *Mol. Biol. Cell 10*, 2126.
3. Vallee, R. B., Williams, J. C., Varma, D., and Barnhart, L. E. (2004) Dynein: An ancient motor protein involved in multiple modes of transport, *J. Neurobiol. 58*, 189−200.
4. King, S. M. (2000) The dynein microtubule motor, *Biochim. Biophys. Acta 1496*, 60−75.
5. Gill, S. R., Cleveland, D. W., and Schroer, T. A. (1994) Characterization of Dlc-a and Dlc-B, two families of cytoplasmic dynein light-chain subunits, *Mol. Biol. Cell 5*, 645−654.
6. Steffen, W., Hodgkinson, J. L., and Wiche, G. (1996) Immunogold localisation of the intermediate chain within the protein complex of cytoplasmic dynein, *J. Struct. Biol. 117*, 227−235.
7. King, S. M., Barbarese, E., Dillman, J. F., Benashski, S. E., Do, K. T., Patel-King, R. S., and Pfister, K. K. (1998) Cytoplasmic dynein contains a family of differentially expressed light chains, *Biochemistry 37*, 15033−15041.
8. Espindola, F. S., Suter, D. M., Partata, L. B. E., Cao, T., Wolenski, J. S., Cheney, R. E., King, S. M., and Mooseker, M. S. (2000) The light chain composition of brain Myosin-Va: Calmodulin, myosin-II essential light chains, and 8-kDa dynein light chain/PIN, *Cell Motil. Cytoskeleton 47*, 269−281.
9. Jaffrey, S. R., and Snyder, S. H. (1996) PIN: An associated protein inhibitor of neuronal nitric oxide synthase, *Science 274*, 774−777.
10. Schnorrer, F., Bohmann, K., and Nusslein-Volhard, C. (2000) The molecular motor dynein is involved in targeting Swallow and the bicoid RNA to the anterior pole of *Drosophila* oocytes, *Nat. Cell Biol. 2*, 185−190.
11. Puthalakath, H., Huang, D. C. S., O'Reilly, L. A., King, S. M., and Strasser, A. (1999) The proapoptotic activity of the Bcl-2 family member Bim is regulated by interaction with the dynein motor complex, *Mol. Cell 3*, 287−296.
12. Kaiser, F. J., Tavassoli, K., van den Bemd, G. J., Chang, G. T. G., Horsthemke, B., Moroy, T., and Ludecke, H. J. (2003) Nuclear interaction of the dynein light chain LC8a with the TRPS1 transcription factor suppresses the transcriptional repression activity of TRPS1, *Hum. Mol. Genet. 12*, 1349−1358.
13. Beckwith, S. M., Roghi, C. H., Liu, B., and Morris, N. R. (1998) The 8-kDa cytoplasmic dynein light chain is required for nuclear migration and for heavy chain localization in *Aspergillus nidulans*, *J. Cell Biol. 143*, 1239−1247.
14. Pazour, G. J., Wilkerson, C. G., and Witman, G. B. (1998) A dynein light chain is essential for the retrograde particle movement of intraflagellar transport (IFT), *J. Cell Biol. 141*, 979.
15. Dick, T., Ray, K., Salz, H. K., and Chia, W. (1996) Cytoplasmic dynein (ddlc1) mutations cause morphogenetic defects and apoptotic cell death in *Drosophila melanogaster*, *Mol. Cell. Biol. 16*, 1966−1977.
16. Boylan, K. L. M., and Hays, T. S. (2002) The gene for the intermediate chain subunit of cytoplasmic dynein is essential in *Drosophila*, *Genetics 162*, 1211−1220.
17. Ye, G. J., Vaughan, K. T., Vallee, R. B., and Roizman, B. (2000) The herpes simplex virus 1 U(L)34 protein interacts with a cytoplasmic dynein intermediate chain and targets nuclear membrane, *J. Virol. 74*, 1355−1363.
18. Karki, S., Ligon, L. A., DeSantis, J., Tokito, M., and Holzbaur, E. L. F. (2002) PLAC-24 is a cytoplasmic dynein-binding protein that is recruited to sites of cell−cell contact, *Mol. Biol. Cell 13*, 1722−1734.
19. Dhani, S. U., Mohammad-Panah, R., Ahmed, N., Ackerley, C., Ramjeesingh, M., and Bear, C. E. (2003) Evidence for a functional interaction between the CIC-2 chloride channel and the retrograde motor dynein complex, *J. Biol. Chem. 278*, 16262−16270.
20. Ligon, L. A., Karki, S., Tokito, M., and Holzbaur, E. L. F. (2001) Dynein binds to β-catenin and may tether microtubules at adherens junctions, *Nat. Cell Biol. 3*, 913−917.
21. Boylan, K., Serr, M., and Hays, T. (2000) A molecular genetic analysis of the interaction between the cytoplasmic dynein intermediate chain and the Glued (dynactin) complex, *Mol. Biol. Cell 11*, 3791−3803.
22. Schroer, T. A. (1996) Structure and function of dynactin, *Semin. Cell Dev. Biol. 7*, 321−328.
23. King, S. J., and Schroer, T. A. (2000) Dynactin increases the processivity of the cytoplasmic dynein motor, *Nat. Cell Biol. 2*, 20−24.
24. Vallee, R. B., Vaughan, K. T., and Echeverri, C. J. (1995) Targeting of cytoplasmic dynein to membranous organelles and kinetachores via dynactin, *Cold Spring Harbor Symp. Quant. Biol. 60*, 803−811.
25. Tai, C. Y., Dujardin, D. L., Faulkner, N. E., and Vallee, R. B. (2002) Role of dynein, dynactin, and CLIP-170 interactions in LIS1 kinetochore function, *J. Cell Biol. 156*, 959−968.
26. Burkhardt, J. K., Echeverri, C., Nilsson, H., and Vallee, R. (1997) Overexpression of the dynamitin (p50) subunit of the dynactin complex disrupts dynein-dependent maintenance of membrane organelle distribution, *J. Cell Biol. 139*, 469−484.
27. Makokha, M., Hare, M., Li, M. G., Hays, T., and Barbar, E. (2002) Interactions of cytoplasmic dynein light chains Tctex-1 and LC8 with the intermediate chain IC74, *Biochemistry 41*, 4302−4311.
28. Wilkerson, C. G., King, S. M., Koutoulis, A., Pazour, G. J., and Witman, G. B. (1995) The 78,000 M(R) intermediate chain of chlamydomonas outer arm dynein Is a wd-repeat protein required for arm assembly, *J. Cell Biol. 129*, 169−178.
29. Vaughan, K. T., and Vallee, R. B. (1995) Cytoplasmic dynein binds dynactin through a direct interaction between the intermediate chains and pl50(Glued), *J. Cell Biol. 131*, 1507−1516.
30. Ma, S., Trivinos-Lagos, L., Graf, R., and Chisholm, R. L. (1999) Dynein intermediate chain mediated dynein−dynactin interaction is required for interphase microtubule organization and centrosome replication and separation in Dictyostelium, *J. Cell Biol. 147*, 1261−1273.
31. Lo, K. W. H., Naisbitt, S., Fan, J. S., Sheng, M., and Zhang, M. J. (2001) The 8-kDa dynein light chain binds to its targets via a conserved (K/R)XTQT motif, *J. Biol. Chem. 276*, 14059−14066.
32. Mok, Y. K., Lo, K. W. H., and Zhang, M. J. (2001) Structure of Tctex-1 and its interaction with cytoplasmic dynein intermediate chain, *J. Biol. Chem. 276*, 14067−14074.
33. Dunker, K. A., Brown, C. J., Lawson, D., Iakoucheva, L. M., and Obradovic, Z. (2002) Intrinsic disorder and protein function, *Biochemistry 41*, 6573−6582.
34. Namba, K. (2001) Roles of partly unfolded conformations in macromolecular self-assembly, *Genes Cells 6*, 1−12.
35. Namba, K., and Stubbs, G. (1986) Structure of tobacco mosaic-virus at 3.6 Å resolution−Implications for assembly, *Science 231*, 1401−1406.
36. Yonekura, K., Maki, S., Morgan, D. G., DeRosier, D. J., Vonderviszt, F., Imada, K., and Namba, K. (2000) The bacterial flagellar cap as the rotary promoter of flagellin self-assembly, *Science 290*, 2148−2152.
37. Nyarko, A., Hare, M., Makokha, M., and Barbar, E. (2003) Interactions of LC8 with N-terminal segments of the intermediate chain of cytoplasmic dynein, *Scientificworld J. 3*, 647−658.

38. Lowry, O. H., Rosebrough, N. J., Farr, A. L., and Randall, R. J. (1951) Protein measurement with Folin Phenol reagent, *J. Biol. Chem. 193*, 265−275.
39. Peterson, G. L. (1983) Determination of total protein concentration, *Methods Enzymol. 91*, 95−119.
40. Andrade, M. A., Chacon, P., Merolo, J. J., and Moran, F. (1993) Evaluation of secondary structure of proteins from UV circular dichroism using unsupervised learning neural network, *Protein Eng. 6*, 383−390.
41. Laemmli, U. K. (1970) Cleavage of structural proteins during the assembly of the head of bacteriophage T4, *Nature 227*, 680−685.
42. Lupas, A., van Dyke, M., and Stock, J. (1991) Predicting coiled coils from protein sequences, *Science 252*, 1162−1164.
43. Wolf, E., Kim, P. S., and Berger, B. (1997) MultiCoil: A program for predicting two- and three-stranded coiled coils, *Protein Sci. 6*, 1179−1189.
44. Jones, D. T. (1999) Protein secondary structure prediction based on position-specific scoring matrices, *J. Mol. Biol. 292*, 195−202.
45. Lau, S. Y., Taneja, A. K., and Hodges, R. S. (1984) Synthesis of a model protein of defined secondary and quaternary structure. Effect of chain length on the stabilization and formation of two-stranded α helical coiled-coils, *J. Biol. Chem. 261*, 10037−10042.
46. Barbar, E., Kleinman, B., Imhoff, D., Li, M. G., Hays, T. S., and Hare, M. (2001) Dimerization and folding of LC8, a highly conserved light chain of cytoplasmic dynein, *Biochemistry 40*, 1596−1605.
47. Tompa, P. (2002) Intrinsically unstructured proteins, *Trends Biochem. Sci. 27*, 527−533.
48. Takano, E., Maki, M., Mori, H., Hatanaka, M., Marti, T., Titani, K., Kannagi, R., Ooi, T., and Murachi, T. (1988) Pig-heart calpastatin—Identification of repetitive domain structures and anomalous behavior in polyacrylamide gel electrophoresis, *Biochemistry 27*, 1964−1972.
49. Yancey, P. H., Clark, M. E., Hand, S. C., Bowlus, R. D., and Somero, G. N. (1982) Living with water stress: Evolution of osmolyte systems, *Science 217*, 1214−1222.
50. Bolen, D. W., and Baskakov, I. V. (2001) The osmophobic effect: Natural selection of a thermodynamic force in protein folding, *J. Mol. Biol. 310*, 955−963.
51. Kumar, R., Baskakov, I. V., Srinivasan, G., Bolen, D. W., Lee, J. C., and Thompson, E. B. (1999) Interdomain signaling in a two-domain fragment of the human glucocorticoid receptor, *J. Biol. Chem. 274*, 24737−24741.
52. Barbar, E., and Hare, M. (2004) Characterization of the cargo attachment complex of cytoplasmic dynein using NMR and mass spectrometry, *Methods Enzymol. 380*, 219−241.
53. Liu, B., Xiang, X., and Lee, Y. R. J. (2003) The requirement of the LC8 dynein light chain for nuclear migration and septum positioning is temperature dependent in *Aspergillus nidulans*, *Mol. Microbiol. 47*, 291−301.
54. Ligon, L. A., Tokito, M., Finkelstein, J. M., Grossman, F. E., and Holzbaur, E. L. (2004) A direct interaction between cytoplasmic dynein and kinesin I may coordinate motor activity, *J. Biol. Chem. 279*, 19201−19208.
55. Susalka, S. J., Nikulina, K., Salata, M. W., Vaughan, P. S., King, S. M., Vaughan, K. T., and Pfister, K. K. (2002) The roadblock light chain binds a novel region of the cytoplasmic dynein intermediate chain, *J. Biol. Chem. 277*, 32939−32946.
56. Wang, L., Hare, M., Hays, T., and Barbar, E. (2004) Dynein light chain LC8 promotes the assembly of the coiled coil domain of swallow protein, *Biochemistry 43*, 4611−4620.

BI048451+